© 2014. Published by The Company of Biologists Ltd | The Journal of Experimental Biology (2014) 217, 2717-2725 doi:10.1242/jeb.101329

RESEARCH ARTICLE

The mechanics and behavior of cliff swallows during tandem flights

Ryan M. Shelton[1], Brandon E. Jackson[1,2] and Tyson L. Hedrick[1,*]

ABSTRACT

Cliff swallows (*Petrochelidon pyrrhonota*) are highly maneuverable social birds that often forage and fly in large open spaces. Here we used multi-camera videography to measure the three-dimensional kinematics of their natural flight maneuvers in the field. Specifically, we collected data on tandem flights, defined as two birds maneuvering together. These data permit us to evaluate several hypotheses on the high-speed maneuvering flight performance of birds. We found that high-speed turns are roll-based, but that the magnitude of the centripetal force created in typical maneuvers varied only slightly with flight speed, typically reaching a peak of ~2 body weights. Turning maneuvers typically involved active flapping rather than gliding. In tandem flights the following bird copied the flight path and wingbeat frequency (~12.3 Hz) of the lead bird while maintaining position slightly above the leader. The lead bird turned in a direction away from the lateral position of the following bird 65% of the time on average. Tandem flights vary widely in instantaneous speed (1.0 to 15.6 m s^{-1}) and duration (0.72 to 4.71 s), and no single tracking strategy appeared to explain the course taken by the following bird.

KEY WORDS: Flight, Kinematics, Maneuverability, Chasing, Turning, Biomechanics

INTRODUCTION

Behaviors in bird, bat and flying insect species range in complexity from migratory cruising to high- and low-speed maneuvering during courtship, territory defense and predator–prey interactions. Our understanding of the maneuverability of bats (Iriarte-Díaz and Swartz, 2008; Riskin et al., 2008) and insects (Card and Dickinson, 2008; Combes et al., 2012), along with birds (Tobalske, 2007), has grown rapidly over the last decade with new methodological developments being deployed in studies across flying species. Most research to date on the mechanics of vertebrate flight has taken place in laboratories with wind tunnels (e.g. Tobalske and Dial, 1996; Ward et al., 2001; Spedding et al., 2003) or simple obstacle courses navigated at low speed (e.g. Swaddle, 1997; Warrick et al., 1998). The latter is a powerful approach for analyzing a specific maneuver because it allows for repeatable behaviors and optimally placed cameras to capture subtle details of the flight movements (e.g. Hedrick and Biewener, 2007; Iriarte-Díaz and Swartz, 2008; Ros et al., 2011). However, the behaviors elicited in laboratory environments may differ from those in natural environments, and are confined in speed and scope by the size of the experimental space. To overcome these difficulties, and to better understand the dynamics of high-speed avian flight maneuvers, we use high-speed video cameras to quantify flight maneuvers and conspecific interactions in natural environments.

We chose to study cliff swallows [*Petrochelidon pyrrhonota* (Vieillot 1817)] because they perform their well-known flight maneuvers in open spaces that permit easy recording with cameras. Cliff swallows build nests in large colonies each spring in North America and migrate to South America for the winter (Brown and Brown, 1986). They are highly social passerines that perform many activities in groups including feeding, preening, gathering mud for nest-building, and perching (Emlen, 1952). As aerial insectivores, cliff swallows have evolved body and wing shapes consistent with changing direction (turning acceleration), and are therefore considered to be highly maneuverable (Brown and Brown, 1998).

Near nesting colonies, cliff swallows engage in one-on-one tandem flights, which appear to be aggressive chase sequences of high-speed maneuvers. These flights have been described as competitive interactions resulting from an intruder approaching a guarded nest (Brown and Brown, 1989). Because cliff swallows are conspecific nest parasites, such chases may serve to prevent the investment of energy in the rearing of adopted offspring (Petrie and Møller, 1991). These tandem flights can escalate to in-flight physical altercations including grappling with their feet, falling from flight while grappling, and disentangling just before reaching the water (R.M.S. and B.E.J., personal observations; see supplementary material Movie 1). Therefore, we expect that the birds participating in tandem flights exhibit flight performance at the upper end of their performance envelope; these interactions appear to include the most elaborate maneuvers at relatively high speeds, compared with other flight behaviors near the nest colony (R.M.S., B.E.J. and T.L.H., personal observations).

This study examines several specific questions related to these free-flight behaviors. What is the performance and maneuvering envelope of freely flying cliff swallows? What are the turning mechanics of cliff swallows in the field? What are the characteristics of these tandem flights? Why do these tandem flights occur? With respect to these questions, we predict that we will see similar linear velocities and accelerations to those previously measured in laboratory-based obstacle courses and wind tunnels (Warrick, 1998; Park et al., 2001), and that roll angle is the primary variable determining the centripetal force and the rate of change in heading because this is the primary method of turning for both airplanes and dragonflies (Alexander, 1986). With regard to bird–bird interactions, we expect that these tandem flights are chases with a simple tracking or intercepting algorithm as exhibited by insects (Collett and Land, 1978; Olberg et al., 2000) because we have seen birds physically fight in midair; and that these tandem flights are competitive interactions, with the lead bird taking action to avoid the following bird because the tandem flights tend to start near the nests in the season of nest guarding (Brown and Brown, 1989).

[1]Department of Biology, University of North Carolina at Chapel Hill, Chapel Hill, NC 27599, USA. [2]Biological and Environmental Sciences, Longwood University, Farmville, VA 23909, USA.

*Author for correspondence (thedrick@bio.unc.edu)

Received 13 December 2013; Accepted 9 May 2014

The Journal of Experimental Biology (2014) doi:10.1242/jeb.101329

List of symbols and abbreviations

a	acceleration (m s^{-2})
AIC	Akaike's information criterion
C_L	coefficient of lift (dimensionless)
F	centripetal force (body weights)
F'	gravity-adjusted centripetal force (body weights)
r	radius of curvature (m)
S	wing area (m^2)
u	flight speed (m s^{-1})
v	velocity (m s^{-1})
w	rate of change in heading (deg s^{-1})
θ	roll angle relative to the horizontal plane (deg)
θ′	roll angle relative to the plane defined by F' (deg)

RESULTS

General results

In each recorded tandem flight, the following bird copied the movements of the lead bird in three-dimensional (3D) space and in the *x*-, *y*- and *z*-position components independently (e.g. Fig. 1). Copying behavior appeared to be independent of variation in distance travelled, interaction time, elevation change and turning rate among tandem flights. We recorded the mean and maximum speed, acceleration, rate of change in heading (here the direction of the 3D velocity vector) and flight time of our trials (Table 1). The mean of the trial mean speeds (7.0 m s^{-1}) is less than half the maximum observed instantaneous speed (15.6 m s^{-1}), showing that these interactions often occur below peak linear speed performance. The mean (±s.d.) power of the 10 trials with the highest mass-specific power was 21.2±4.5 W kg^{-1} (see Eqn 1 in the Materials and methods). These tandem flights were short, lasting 2.28 s on average.

Turning performance

We measured or calculated the roll angle relative to the centripetal force (θ′), flight speed (u), rate of change in heading (w) and gravity-adjusted centripetal force (F') of 42 lead bird turns, and found strong and significant correlations between gravity-adjusted roll angle (θ′) and w (r^2=0.727, P<0.001; Fig. 2A), θ′ and adjusted centripetal force (F') (r^2=0.876, P<0.001; Fig. 2B), and F' and w (r^2=0.746, P<0.001; Fig. 2C). We did not find a significant correlation between u and F' (r^2=0.085, P=0.065; Fig. 2D), and found only a weak association between u and w (r^2=0.111, P=0.031). There was one turn with an apparent F' outlier producing 7.8 body weights of force, more than twice the force of any other observed turn, which was not included in the above statistics – see further examination of this result below. The extended mixed-effects analysis of these results (supplementary material Table S1) confirmed the findings of the linear regressions: a linear model relating F' to θ′ produced the lowest Akaike's information criterion (AIC) of all models without random effects (84.08), and the overall best model added a random effect of trial but only reduced the AIC to 82.04; the linear coefficient for θ′ was highly significant and nearly identical in the two cases.

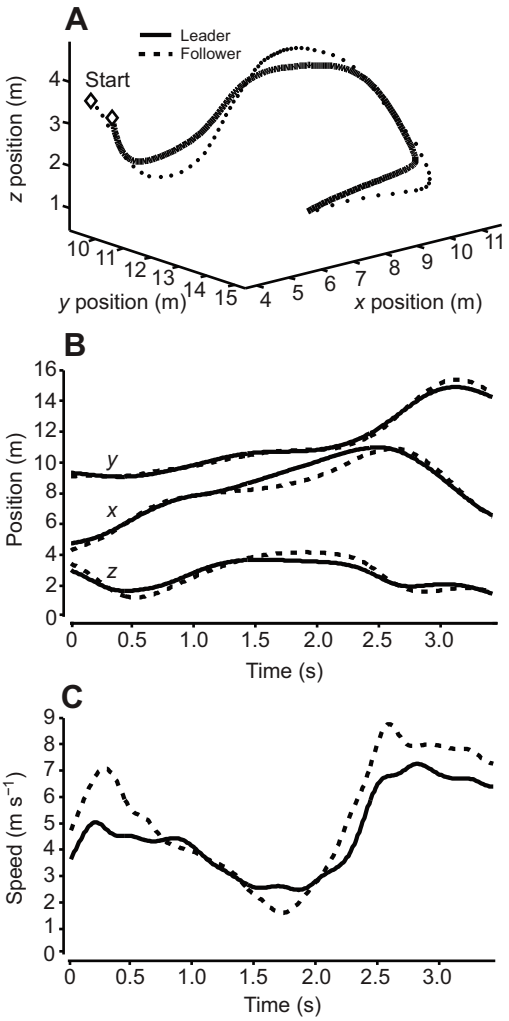

Fig. 1. Here, we show typical trajectory kinematics for a tandem flight recording. (A) The 3D positions of a lead and following bird for a tandem flight starting at the diamonds in the upper left. The *z*-axis is aligned with gravity. (B) The *x*, *y* and *z* components of the position with respect to time. The following bird copies the lead bird's position closely in each component. (C) The speed of the following bird is slightly faster than the lead bird and the speed in this tandem flight ranges from 1.6 to 8.8 m s^{-1}.

Leader–follower comparisons

We observed a variety of following positions with respect to the lead bird, but there was a tendency to avoid following directly behind the leader (Fig. 3A), and a statistically significant trend of aiming above the leader (using a generalized estimating equation, P=0.03; Fig. 3B).

The mean wingbeat frequencies of the lead bird (12.3±1.7 Hz) and the following bird (12.4±1.6 Hz) were statistically indistinguishable. The following bird, on average, started its downstroke less than one-fourth of a wingbeat after the lead bird (Fig. 4). In Fig. 4, the outer circle represents the full wingbeat cycle

Table 1. Flight performance

Variable	Instantaneous maxima	Mean of trial means	Standard deviation of means
Speed (m s$^{-1)}$	15.6	7.0	2.4
Acceleration (m s$^{-2)}$	78.1	13.6	6.6
Magnitude of rate of change in heading, w (deg s^{-1})	642	107	37
Tandem flight time (s)	4.71	2.28	1.14

The Journal of Experimental Biology (2014) doi:10.1242/jeb.101329

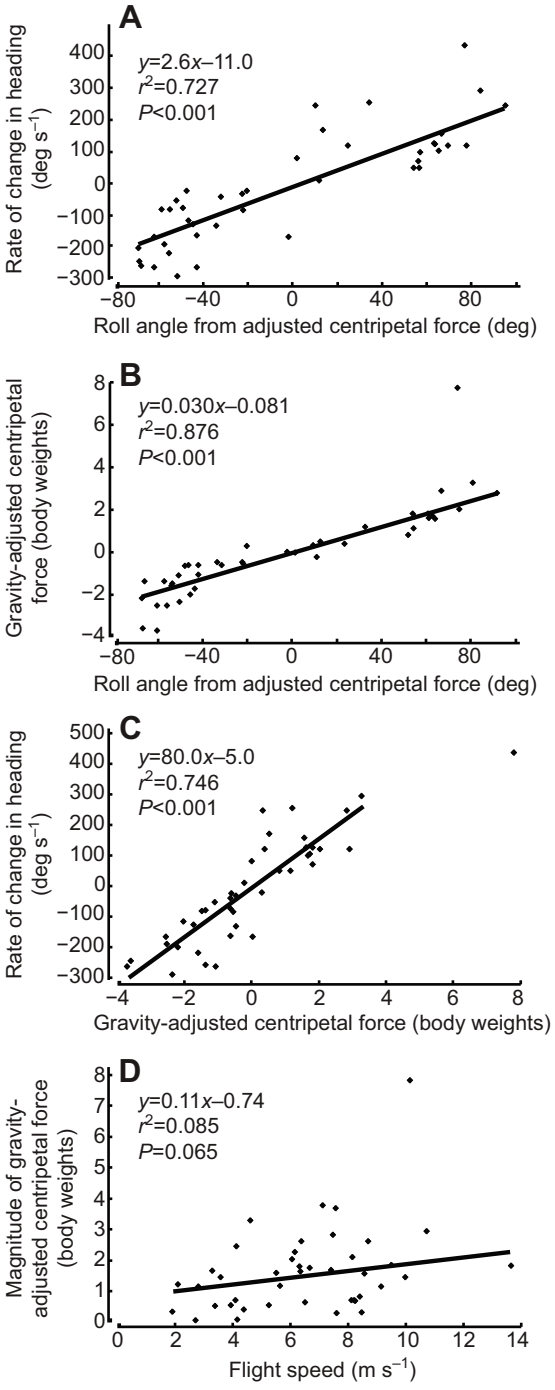

Fig. 2. Here, we document relationships between several maneuvering kinematic metrics. For 42 turns we compared (A) rate of change in heading with respect to the roll angle relative to the gravity-adjusted centripetal force, (B) gravity-adjusted centripetal force with respect to roll angle relative to the gravity-adjusted centripetal force, (C) rate of change in heading with respect to gravity adjusted centripetal force, and (D) flight speed with respect to gravity-adjusted centripetal force. For roll angle with respect to gravity-adjusted centripetal force, rate of change in heading, and gravity-adjusted centripetal force, positive=right and negative=left. A–C have high correlations and significant *P*-values, but D has a near-zero correlation and is insignificant. The equations and statistics do not include the centripetal force outlier of 7.8 body weights.

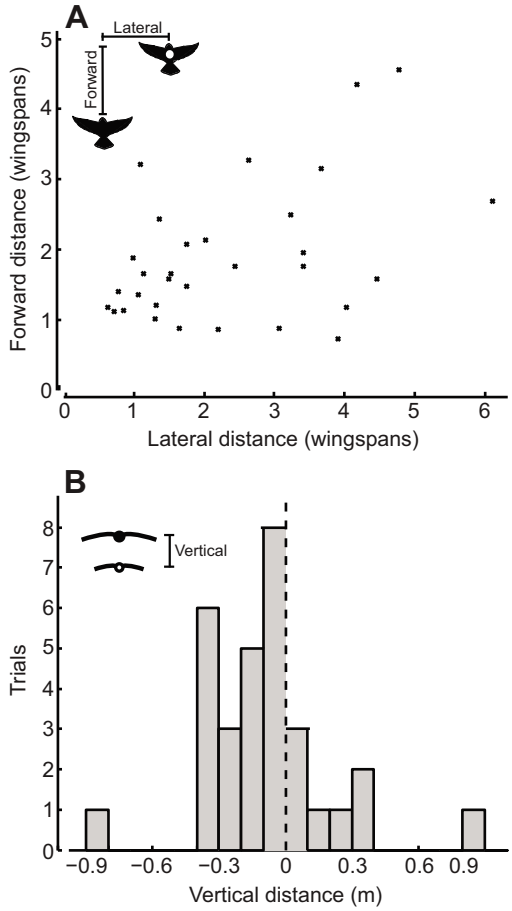

Fig. 3. Here, we examine horizontal and vertical spatial organization among swallows. (A) Each marker represents the mean location of the lead bird with respect to the following bird through one entire tandem flight sequence (*n*=31). (B) The histogram shows the mean vertical location of the leader for each trial with negative distances defined by the leader being below the follower's trajectory. The dashed line at zero shows the expected mean if the follower was aiming in line with the leader. This distance is significantly less than zero using a generalized estimating equation with *P*=0.03, meaning the follower tends to aim above the leader.

of the following bird and each point is the mean timing of the start of the downstroke of the lead bird. Perfect synchronization would be represented by all points positioned at 0 deg. The non-random distribution (Rayleigh test; r=0.38, P=0.021, n=26) averaged 332 deg (95% CI: 292 to 11 deg).

On average, the lead bird turned away from the following bird for 65% of the tandem flight (*t*-test, P<0.001; Fig. 5A). The following bird had a longer flight path and flew 6% faster on average than the lead bird (*t*-test, P≤0.001; Fig. 5B).

High force outlier

We estimated a centripetal force of 7.8 body weights in one turn, more than double any other turn we observed (Fig. 6). This sequence included a number of factors that may have contributed to the high force measurement: a large θ of 78 deg, a fast speed of 14.6 m s^{-1} immediately preceding the turn, a quick reduction in speed by 4.5 m s^{-1} during the time of the turn, and the possibility of ground effect enhancing aerodynamic forces because the entire tandem flight occurred just above the water surface.

DISCUSSION

Flight performance envelope

Compared with the single turn produced by 7.8 times body weight force, most trials included performance well within the known flight

The Journal of Experimental Biology (2014) doi:10.1242/jeb.101329

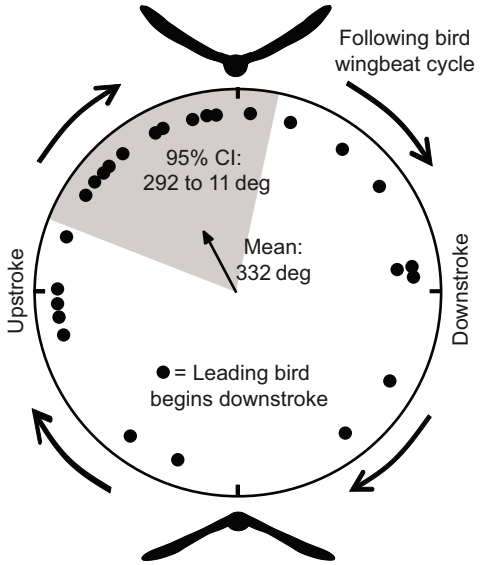

Fig. 4. The phase offset of the beginning of downstroke among the follower and the leader. The outer circle represents the full wingbeat cycle of the following bird. For each wingbeat cycle we observed the timing in frames of the start of the lead bird's downstroke relative to the following bird's wingbeat cycle. Each circle is the mean timing of the start of the lead bird's downstroke for a single trial. If the top of this graph is defined as 0 deg and numbers increase clockwise, the mean of the trial means is 332 deg (r=0.38, P=0.021, n=26) with the shaded region showing the 95% confidence interval. This is a significant result, supporting a non-random distribution of wingbeat phasing between the two birds with the lead bird tending to flap just before the following bird.

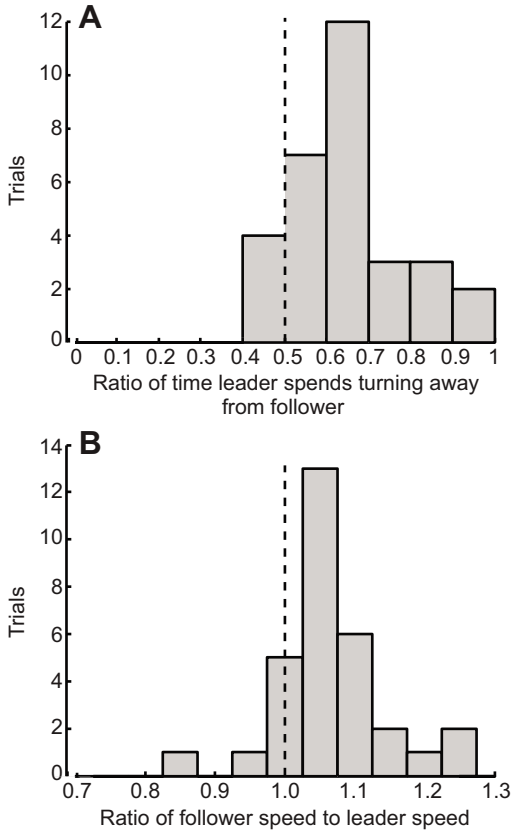

Fig. 5. The lead bird tends to turn away from the following bird causing the following bird to fly slightly faster to maintain position. (A) For each trial we measured the ratio of time that the lead bird is turning away from the following bird and found the leader turning away for the majority of time in 27 of 31 trials. The dashed line at 0.5 shows the expected mean if the turn direction was random. The data mean is significantly different from 0.5 (mean = 0.65, s.e.m. = 0.03; t-test, P<0.001). (B) The ratio of the mean followers speed to mean leaders speed shows that the lead bird is flying faster than the following bird in only two of 31 trials, suggesting that the following bird is flying faster to adjust to an unpredictable flight path. The dashed line at 1.0 shows the expected mean if both birds had the same mean velocity. These data are significantly different from 1.0 (mean = 1.06, s.e.m. = 0.01; t-test, P<0.001).

envelope for cliff swallows and related species. Although to the best of our knowledge cliff swallow flight has not been examined in a wind tunnel, we can compare our data with previous research on barn swallows (*Hirundo rustica*). Flight speeds of two barn swallows ranged from 3.4 to 14.0 m s^{-1} in a wind tunnel (Park et al., 2001). We found that the time-averaged flight speeds of cliff swallows had a similar range and identical maximums (2.8 to 14.0 m s^{-1}) despite differences in wing shape and body size between the two species. Because we measured open-area flights and birds were free to fly at self-chosen varying speeds, we can also look at the maximum instantaneous flight speeds over 0.01 s intervals. Cliff swallows flew at instantaneous speeds up to 15.6 m s^{-1}.

Cliff swallows have been previously examined during linear escape flights. Warrick found that the linear acceleration in four different swallow species ranged from 5.45 to 8.92 m s^{-2}, with cliff swallows averaging 5.98 m s^{-2}, when measured starting from rest and flying in a straight horizontal line (Warrick, 1998). Cliff swallows in tandem flights had an average linear acceleration of 13.6 m s^{-2}, but unlike the horizontal flight test experiment, some of the swallows in our study were able to descend, using potential energy as well as muscle work to accelerate, and potentially taking advantage of other environmental factors. Calculating the mass-specific power output (not including drag; see Eqn 1) can account for added acceleration due to gravity and provides a more relevant comparison between the different behaviors. Warrick's cliff swallows started from rest and accelerated to 7.26 m s^{-1} in 4 m, resulting in a mass-specific power of 22.8 W kg^{-1} (23 g body mass). Swallows in tandem flights, starting from a wide range of speeds, averaged 21.2±4.5 W kg^{-1} (mean ± s.d.). These power estimates would increase if we included drag and a full aerodynamic model. Thus, the freely flying swallows exhibited approximately the same mass-specific power as was found in the capture and release study of escape accelerations, even though the conditions of these measurements were drastically different. The level acceleration experiment with recently captured wild swallows was designed to elicit maximum performance; the similar results from freely behaving birds suggest that cliff swallows may use most, if not all, of their performance envelope on a day-to-day basis.

The vertical take-off power outputs of blue-breasted quail [47.0 W kg^{-1}; 43.6 g body mass (Askew et al., 2001)] and gray jay [27.7 W kg^{-1}; 68.9 g body mass (Jackson and Dial, 2011)] are larger than our measured cliff swallow free-flight power. Assuming morphological isometry, aerodynamic and allometric theory would predict that the smaller cliff swallows should have higher mass-specific power outputs than the other, larger species (Pennycuick, 1975), which may suggest that our cliff swallow values are not maximal. Alternately, because swallows are not acceleration specialists and can often use potential energy to enhance flight maneuvers and prey capture attempts, cliff swallows may simply have a lower maximal capability for muscle-powered acceleration.

Based on the flight speed and turning radius in tandem flight turns, we estimated the aerodynamic centripetal forces developed by

The Journal of Experimental Biology (2014) doi:10.1242/jeb.101329

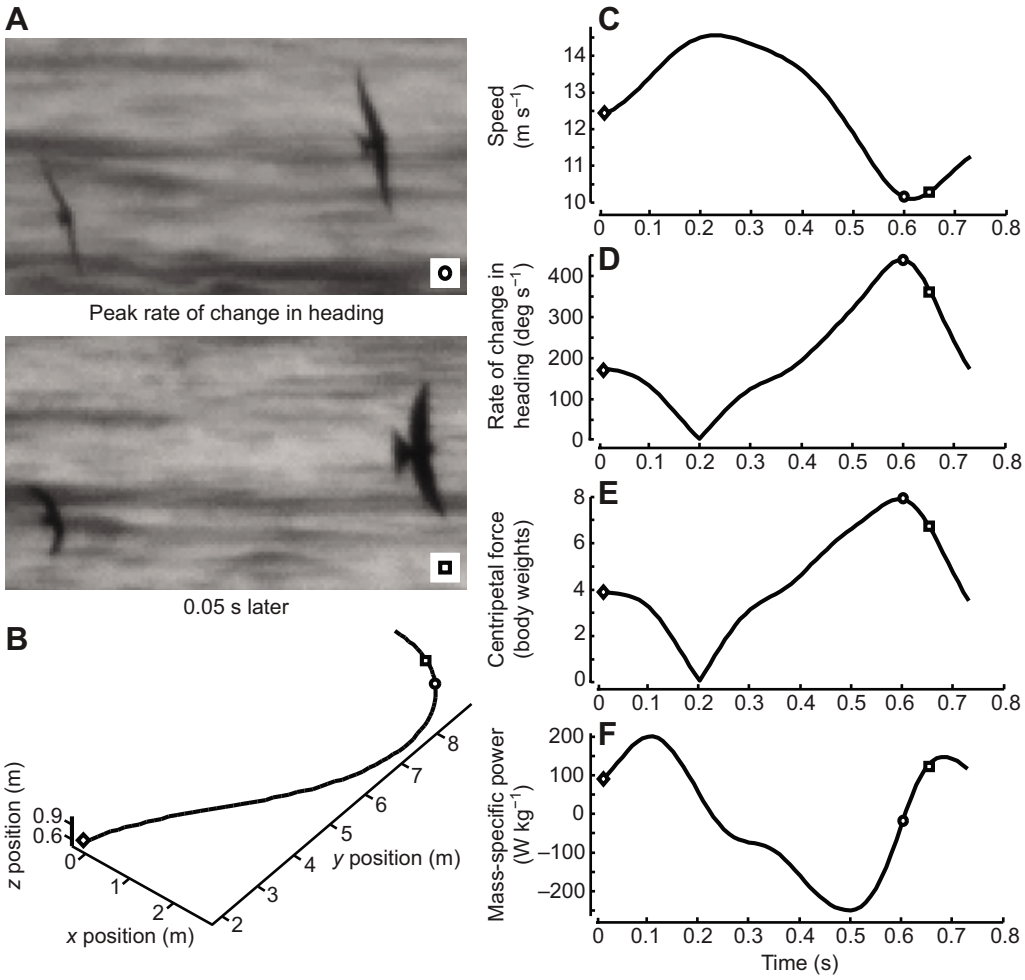

Fig. 6. This lead bird turn had a centripetal force twice as large as any other observed turn, and a rate of change in heading 35% larger than any other turn. (A) The moment of peak rate of change in heading, and the moment 0.05 s later. The circle and square markers in the lower right corners are presented in the graphs to show the timing of these images. The contrast in these images has been enhanced. The 3D position (B), velocity with respect to time (C), rate of change in heading (D), centripetal force (E) and mass-specific power (F) are presented with each sequence starting at the diamond. The lead bird starts climbing around 0.5 s, producing an increase in potential energy, which causes the mass-specific power to reach a minimum prior to the minimum speed.

cliff swallows (Table 1, Fig. 2). Similar field measurements during high-speed flight have only been reported for the courtship dives of Anna's hummingbirds, which experienced a gravity-assisted centripetal force of 9 body weights on average while reaching an average maximum flight speed of 27.3 m s^{-1} (Clark, 2009). This centripetal force is only slightly higher than the 7.8 body weights maximum reported here, but much greater than our median magnitude of centripetal force of 1.0 body weights. The static wingload of adult male Anna's hummingbirds is 28.8 Pa [converted from 0.294 g cm^{-2}; 4.3 g body mass (Stiles et al., 2005)], or roughly 60% larger than that of cliff swallows at 18.0 Pa (Warrick, 1998). Thus, Anna's hummingbirds appear to be producing higher centripetal forces with respect to both body weights and wingloads, albeit at a flight speed approximately twice that of the cliff swallows. This difference is not surprising considering the large difference in ecological niche and typical flight behavior of these birds. It is likely that the number of documented turning kinematics in the literature will rapidly increase over the next 10 years, providing more of a scaling context for these results.

We can also compare these centripetal forces with experiments on pigeons and cockatoos completing 90 deg turns through L-shaped corridors at low speeds in laboratory maneuvering tests. Pigeons flying at 3.3 m s^{-1} with a turning radius of ~1.0 m produced a maneuver-averaged centripetal force of 10.9 body weights (Ros et al., 2011); rose-breasted cockatoos making similar turns at 3.01 m^{-1} with a radius of 0.92 m produced 9.8 body weights (Hedrick and Biewener, 2007). These larger birds are producing larger forces than our cliff swallows, which produced less than 2.0 body weights at similar speeds and likely reflect the severe spatial constraints the birds were forced to maneuver under in the laboratory studies.

Turning mechanics

As we predicted, θ' strongly correlated with both F' and w. Swallows produced approximately 2.7 body weights of centripetal force at a 90 deg θ' (Fig. 2B), independent of flight speed (Fig. 2D). An ideal fixed-wing glider performing a level turn could transfer all aerodynamic force (lift) into centripetal force and would be able to produce 1.0 body weights of centripetal force at a 90 deg roll angle, assuming no change in coefficient of lift. These differences are reasonable given the swallows' expected ability to vary coefficient of lift and their continued wing flapping through most of the turns. We were unable to determine many details of wing flapping kinematics such as wing extension, stroke amplitude and gait changes.

The basic mechanics of the cliff swallow turns were different from those expected for a fixed-wing glider. In the Materials and methods we derive a simple linearized expression for a simple fixed-wing banked turn to $F' \propto \theta'$ (Eqn 9). Stepping back two equations in our model to $F' \propto u^2\sin(\theta')$ (Eqn 7), we expected to see our correlations increase. Instead, when we substituted any combination of u, u^2, $\sin(\theta')$ or $\tan(\theta')$ for θ', our correlations decreased in strength (see supplementary material Table S1). When we tried substituting the horizontal component of centripetal force [$F'\cos(\theta')$] for F' we also saw a decrease in correlations. Essentially, the lateral force produced by swallows is proportional to roll angle, indicating a banked turn, but nearly independent of forward velocity.

This indicates that swallows rarely use large lift coefficients when turning while flying fast, despite their apparent ability to do so as demonstrated by the 7.8 ***g*** turn discussed earlier. In that maneuver the bird also slowed rapidly, presumably because of the induced drag associated with the large lift coefficient, demonstrating the costs of high force turns. Furthermore, flapping provides another avenue for producing larger forces than expected from forward speed alone and could also account for the absence of a forward speed relationship, especially at slow speeds. The majority of turns recorded here were flapping maneuvers. The absence of improvement when using sin(θ′) or tan(θ′) to examine a specific lift-based turn model, where the bird either produces no additional force or produces additional force adequate to maintain perfect weight support, suggests that swallows may compromise between the two, producing some additional force but not enough for weight support at larger θ′, a result also supported by the magnitude of the linear coefficient relating θ′ to F'. Finally, our large filming volume precluded us from being able to discern detailed wingbeat kinematics; higher resolution or closer image captures of swallows turning in high-speed free flight will be necessary to detail the exact motions of the swallow wings and body that produce F'.

Tandem flights

Our initial hypothesis that all of these tandem flights were chases including a simple tracking or intercepting strategy was not supported. Instead of aiming at or in front of the lead bird, the follower tends to fly parallel to the lead bird while offset to one side or the other, with the result that the following bird generally copies the flight path of the lead bird. These data do not support the assumption that the following bird had the 'goal' of making contact with the lead bird, although we occasionally did see contact between two birds (e.g. supplementary material Movie 1). However, the tendency of the lead bird to turn away from the follower and for the follower to fly faster than the leader (Fig. 5) does support the hypothesis that these flights are competitive interactions. Cliff swallows live in highly cooperative populations but they also have high intraspecific brood parasitism (Brown and Brown, 1989), which could invoke competitive interactions. The flights we recorded mostly occurred in May and early June, coinciding with nest building and egg laying. Additionally, although we could not determine the location of the birds relative to the home nest, most of the flights began close to nests (R.M.S. and B.E.J., personal observation), further suggesting that these tandem flights were acts of nest defense from conspecifics. The large variation in speed, length, bird position and turning behaviors among trials may represent varying degrees of relative competitiveness of the two birds involved, with some birds being driven away more easily and other birds requiring more aggressive pursuit. The offset position of the follower may provide an aerodynamic advantage of reducing flight cost (Portugal et al., 2014), or a behavioral advantage of allowing the follower to be seen or to cut off turns towards the nest. These tandem flights might be a graded display with the threat of escalation to physical combat. If so, the birds would attempt to send signals to resolve the conflict with minimal energy loss, which would explain why most turns are well below the maximum observed turning force because producing that maximal force appears to have imposed a substantial cost in induced drag, reflected as a decrease in speed during the turn (Fig. 6).

Wingbeat frequency and the timing of wingbeat cycles were unexpectedly synchronized, with a slight phase shift, in lead and following birds. Because the following bird is copying the lead bird's maneuvers and flight path, it makes sense that the follower would delay its wingbeat in order to first observe the leader's maneuver. On average, our data show the lead bird starting its downstroke 332 deg into the follower's wingbeat cycle (Fig. 4). In other words, the follower's wingbeat starts 28 deg, or ~6 ms, after the leader's wingbeat cycle. This response time is fast in comparison to that of dragonflies [29 ms (Olberg et al., 2007)], hoverflies [~20 ms (Collett and Land, 1978)], houseflies [~30 ms (Land and Collett, 1974)], dolichopodid flies [~15 ms (Land, 1993)] and bats [120 ms (Ghose et al., 2006)]. Thus, it is unlikely that the following birds were simply responding to the timing of the lead birds' downstroke with each wingbeat cycle. Alternatively, the follower may be reacting to whole-body movements of the lead bird, and may require slightly more than the duration of a wingbeat cycle (81 ms total for wingbeat plus 6 ms delay) to receive, interpret and react to the input. In other words, the follower's latency of reaction may mean that what we see as a phase shift of ~30 deg may actually be a phase shift of ~390 deg. If the follower exhibited a consistent tracking strategy we would be able to distinguish between the two phase offset possibilities by extracting the response latency between the leader and follower. However, because the swallows appear to use different tracking strategies depending on context, we cannot use this information to conclusively separate the two possibilities, although a 390 deg offset is more consistent with typical sensory response times as noted above.

MATERIALS AND METHODS

Swallow recordings

We recorded cliff swallow interactions from a colony of 30 to 60 birds at the North Carolina Highway 751 bridge over Jordan Lake, Chatham County, NC, USA (35°49′42″N, 78°57′51″W). We recorded on 26 separate mornings in May and June 2012 and May 2013 collecting 100 Hz 3D kinematic data for 31 tandem flights totaling 71 s. Each day we had a slightly different camera setup and recorded one to three good trials. We are unable to confirm that each trial involved different individuals because we could not identify individual birds. However, we chose to treat each tandem flight as an independent event given the number of birds present at the colony and the elapsed time between trials.

To collect 3D field flight data in large outdoor volumes, we developed a structure-from-motion camera calibration routine that used a wand of known length to set the scale of the scene and provide an initial calibration; this was implemented as a custom MATLAB (The MathWorks, Natick, MA, USA) routine (Therialt et al., 2014). This preliminary calibration was then refined by adding individual swallows from calibration recordings as points of optical correspondence and applying a bundle adjustment optimization (Lourakis and Argyros, 2009) to the data and camera coefficients. The scene was then aligned to gravity by measuring the acceleration of a rock tossed through the scene, transforming the coefficients to place this acceleration vector on the z-axis, and converted to a set of direct linear transformation coefficients for 3D analysis of bird trajectories (Hedrick, 2008). Camera recording positions varied slightly among trials, but typically set a recording volume of ~7000 m^3. Video data were collected using three synchronized high-speed cameras (N5r, Integrated Design Tools, Inc., Tallahassee, FL, USA) recording 2336×1728 pixel images at 100 Hz. The calibrations had a median direct linear transformation residual of 1.23 pixels and the bird trajectories had a median 95% confidence interval of 0.057 m with a range of 0.010 to 0.412 m, where recordings closer to the cameras are more precisely quantified (Therialt et al., 2014).

We minimized the influence of wind by recording on days with little or no wind (<1.5 m s^{-1}). We measured the wind by placing a digital anemometer (HHF142, OMEGA Engineering, Inc., Stamford, CT, USA) on the shoreline near the camera locations elevated between 2 and 6 m above the water level. The anemometer was mounted on a gimbal, allowing free rotation about the vertical axis; wind velocity was recorded at 1 Hz using a custom data logger that sampled the anemometer output, compass direction via a digital magnetometer, and Global Positioning System location and time.

The Journal of Experimental Biology (2014) doi:10.1242/jeb.101329

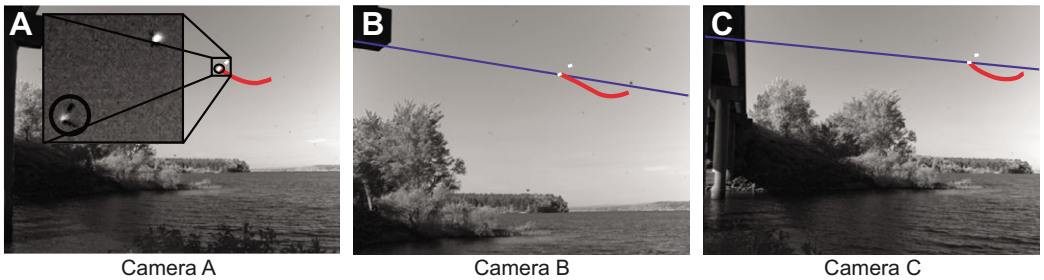

Fig. 7. Example frames from the three synchronized cameras (A–C) placed along the shoreline to capture different views of the same volume of space. After completing our camera calibration procedure, we digitized the location of a bird in two or more camera views, shown here with the bird located in one camera (marked by the black circle in A) and the epipolar lines (in blue in B and C), to find the exact 3D location of the bird at that time. The epipolar line defines the ray where the bird could be located in B and C given its location in A. The zoomed insert in A is contrast enhanced. White areas mark the location of the two digitized birds. The red lines show the flight path of the digitized bird over the preceding 1 s.

Kinematic analysis

We manually digitized the head of each bird in each frame of each camera to determine the 3D bird positions with respect to time for each trial (Fig. 7) using the MATLAB package DLTdv5 (Hedrick, 2008). Each trial includes two birds flying as a pair, with one bird leading and the other bird following. We designate these birds as the lead bird and the following bird, respectively, throughout the paper. These raw data were first processed by iteratively increasing the error tolerances of a quintic smoothing spline to affect a low-pass filter at 1.0, 1.5 and 2.5 Hz to remove digitizing errors and within-wingbeat fluctuations in velocity and acceleration. The error variance was extracted from the 3D reconstruction uncertainty for each data point. Varying the filter did not impact any of our statistical conclusions and introduced only small variations in the data. Results in this paper are from the 1.5 Hz low-pass filter unless otherwise noted. Derivatives of position with respect to time were calculated from the quintic spline polynomial; we examined the first and second derivatives – velocity (**v**) and acceleration (**a**).

We used the filtered position, **v** and **a** data for all further calculations. We recorded the maximum instantaneous values from all of the data for speed, **a** and magnitude of rate of change in heading to document the maximum observed performance (Table 1). We calculated the mass-specific power (not including drag) by:

$$\frac{\text{Power}}{\text{Mass}} = \frac{\Delta\left(\text{Kinetic energy} + \text{Potential energy}\right)}{\text{Time} \times \text{Mass}}. \quad (1)$$

Mass on the right side of this equation will cancel, allowing us to complete the calculation without knowing the mass of the birds. Because our swallows were not always maximizing power, we measured power over each possible 1 s interval for all of our trials and selected the largest mass-specific power from each trial. We then focused on the 10 trials with the largest power for further analysis.

We calculated the instantaneous radius of curvature (r) directly from **v** and **a** by:

$$r = \frac{|\mathbf{v}|^3}{\sqrt{|\mathbf{v}|^2|\mathbf{a}|^2 - (\mathbf{v}\mathbf{a}')^2}}, \quad (2)$$

where $\mathbf{a}'$ is the transpose of **a**. We then calculated rate of change in heading (w) by:

$$w = \frac{u}{r}, \quad (3)$$

with u defined as flight speed. We extracted the frame and trial number of each local maxima in the graph of w with respect to time of the lead birds (number of peaks = 144) and tried to digitize the location of the extended wingtips in that frame (±2 frames) to calculate roll angle (θ). We calculated θ as the angle between the line connecting the two wingtips and the line from one wingtip in the direction of the other wingtip but parallel to the horizontal plane. We could only clearly identify the wingtip locations for 42 of the 144 turns. For these 42 turns we calculated centripetal force (F) in body weights by:

$$F = \frac{u^2}{9.81r}. \quad (4)$$

We added a directional sign (positive = right, negative = left) for w, θ and F.

To evaluate the relative body positions of the lead bird with respect to the following bird, we defined a second non-inertial coordinate system (x_b, y_b, z_b) that rotates with each frame, with x_b remaining perpendicular to gravity. We rotated and shifted the original coordinate axes (x, y, z) to place the following bird at the origin flying up the y_b-axis for each video frame. This allowed us to use the lead bird's coordinates to define the forward distance as the y_b-coordinate, the vertical distance as the z_b-coordinate and the lateral distance as the perpendicular distance from the y_b-axis to the lead bird position (Fig. 8).

We calculated the average wingbeat frequency by visually determining the frame number that each bird had its wingtips at their highest point for each wingbeat cycle. Of our 31 tandem flights, only 26 recordings clearly showed at least four consecutive wingbeats for both birds. To evaluate the relative timing of wingbeats of the lead bird and the following bird, we first evaluated each wingbeat separately. For each following bird wingbeat we calculated the number of frames until the next wingbeat started, set this wingbeat length equal to 360 deg and noted the timing of the start of the lead bird's downstroke relative to the following bird's 360 deg wingbeat. For each trial we took the average timing of the lead bird's downstroke and treated the means from the 26 trials as independent data points.

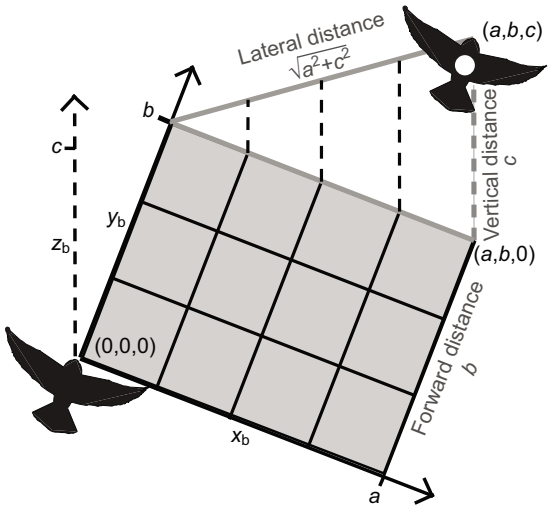

Fig. 8. To measure the lateral, vertical and forward distances between the lead and following birds, we made a non-inertial coordinate system that rotates with each frame with x_b remaining perpendicular to gravity. We shifted and rotated the 3D axes of each frame so the following bird was at the origin flying along the y_b-axis. The vertical distance is the z_b-coordinate of the lead bird (c). The lateral distance is the perpendicular distance from the y_b-axis to the lead bird ($\sqrt{a^2+c^2}$). The forward distance is the y_b-coordinate of the lead bird (b).

Flight model

To test whether roll angle was the primary variable determining the centripetal force and the rate of change in heading, we tested our measurements of F against simplified force models for simple fixed-wing banked turns. We made progressively simplifying assumptions to isolate individual mechanisms. We started with:

$$\text{Lift} = \tfrac{1}{2} C_L S u^2 , \quad (5)$$

where C_L is the lift coefficient and S is wing area. This gives the lateral force F as:

$$F = \tfrac{1}{2} C_L S u^2 \sin(\theta) . \quad (6)$$

If we drop $\frac{1}{2}C_L S$ from the equation by assuming that swallows use a similar lift coefficient and wing area among all maneuvers, we are left with:

$$F \propto u^2 \sin(\theta) . \quad (7)$$

Alternatively, if cliff swallows modulate wing area and lift coefficient to match lift (i.e. vertical force) to body weight and maneuver only by redirecting lift, we expect:

$$F \propto \sin(\theta) , \quad (8)$$

and thus lift proportional to θ after further linearization:

$$F \propto \theta . \quad (9)$$

As a third alternative, cliff swallows may turn by redirecting their lift inward but also modulate coefficient of lift and wing area to maintain a vertical component equal to body weight. In this circumstance:

$$F \propto \tan(\theta) , \quad (10)$$

which also linearizes to Eqn 9 for small θ. Thus, in our simplest model we would expect to see a correlation for F with respect to θ. We would also expect this correlation to increase when we substitute some combination of u, u^2, and sin(θ) or tan(θ) for θ, moving toward the more complete models. Also, we would expect an improved correlation from substituting the horizontal component of centripetal force [by $F\cos(\theta)$] for F.

These simplified equations only characterize turns in the 2D plane perpendicular to gravity and do not include the 3D complexity of the observed turns, which may not be level and may have a gravitational contribution to or against F. These factors were accommodated by subtracting the gravitational contribution from the observed centripetal force vector, resulting in an aerodynamic centripetal force vector F', and measuring the adjusted roll angle θ′ relative to the plane-defined F'. If cliff swallows are using roll-based turns, we would expect to see a correlation between F' and θ′. If the swallows do not change overall lift production during maneuvers, we would expect the coefficient relating θ′ to F' to be ~1.0. The expectations in the above paragraph are still valid after we plug in θ′ to F' for θ to F.

Statistical analysis

We used several different statistical methods to evaluate our data. To measure the correlations between each paired combination of F', θ′, w and u (Fig. 2) we calculated a linear regression, a correlation coefficient (r^2) and a P-value. We used a t-test to evaluate the null hypothesis that the lead bird spends equal amounts of time turning toward and away from the following bird. A t-test was also used to evaluate the null hypothesis that the lead bird and following bird have equal mean velocities. We used MATLAB for these statistics, treating each tandem flight as a single independent trial. We further examined the effect of recording date and trial on the results and additive linear models containing several of the terms from Eqns 7–10 using linear mixed effect models compared by AIC. This analysis was performed in R 2.12 using the nlme package (Pinheiro et al., 2010; R Development Core Team, 2010). A single outlier point with centripetal force more than twice that of the next largest value recorded was excluded from the data for the AIC analysis but not in the initial linear regressions.

To evaluate the relative vertical distance, defined by z_b in Fig. 8, we used a generalized estimating equation to test the null hypothesis that the vertical distance is equal to 0 using R with the geepack library (R Foundation for Statistical Computing, Vienna, Austria) (Zeger et al., 1988). We evaluated the relative wingbeat timing for the lead bird and the following bird using a Rayleigh test in Oriana (Kovach Computing Services, UK) (Brazier, 1994).

Acknowledgements

We wish to thank Nick Deluga, Katherine Sholtis and Amanda Lohmann for their assistance in collecting and analyzing the video data, and members of the Hedrick lab group for valuable discussion. Comments from two anonymous referees resulted in substantial improvements to the paper.

Competing interests

The authors declare no competing financial interests.

Author contributions

The overall experimental concept was developed by T.L.H., data recording and analysis was carried out by R.M.S. and B.E.J. with contributions from T.L.H., and R.M.S. and T.L.H. prepared the manuscript.

Funding

This work was funded by the Office of Naval Research [MURI N000141010952 to T.L.H. and eight others] and by the National Science Foundation [IOS-1253276 to T.L.H.].

Supplementary material

Supplementary material available online at
http://jeb.biologists.org/lookup/suppl/doi:10.1242/jeb.101329/-/DC1

References

Alexander, D. E. (1986). Wind tunnel studies of turns by flying dragonflies. *J. Exp. Biol.* **122**, 81-98.

Askew, G. N., Marsh, R. L. and Ellington, C. P. (2001). The mechanical power output of the flight muscles of blue-breasted quail (*Coturnix chinensis*) during take-off. *J. Exp. Biol.* **204**, 3601-3619.

Brazier, K. T. S. (1994). Confidence intervals from the Rayleigh test. *Mon. Not. R. Astron. Soc.* **268**, 709-712.

Brown, C. R. and Brown, M. B. (1986). Ectoparasitism as a cost of coloniality in cliff swallows (*Hirundo pyrrhonota*). *Ecology* **67**, 1206-1218.

Brown, C. R. and Brown, M. B. (1989). Behavioural dynamics of intraspecific brood parasitism in colonial cliff swallows. *Anim. Behav.* **37**, 777-796.

Brown, C. R. and Brown, M. B. (1998). Intense natural selection on body size and wing and tail asymmetry in cliff swallows during severe weather. *Evolution* **52**, 1461-1475.

Card, G. and Dickinson, M. (2008). Performance trade-offs in the flight initiation of *Drosophila*. *J. Exp. Biol.* **211**, 341-353.

Clark, C. J. (2009). Courtship dives of Anna's hummingbird offer insights into flight performance limits. *Proc. Biol. Sci.* **276**, 3047-3052.

Collett, T. S. and Land, M. F. (1978). How hoverflies compute interception courses. *J. Comp. Physiol.* **125**, 191-204.

Combes, S. A., Rundle, D. E., Iwasaki, J. M. and Crall, J. D. (2012). Linking biomechanics and ecology through predator-prey interactions: flight performance of dragonflies and their prey. *J. Exp. Biol.* **215**, 903-913.

Emlen, J. T. (1952). Social behavior in nesting cliff swallows. *Condor* **54**, 177-199.

Ghose, K., Horiuchi, T. K., Krishnaprasad, P. S. and Moss, C. F. (2006). Echolocating bats use a nearly time-optimal strategy to intercept prey. *PLoS Biol.* **4**, e108.

Hedrick, T. L. (2008). Software techniques for two- and three-dimensional kinematic measurements of biological and biomimetic systems. *Bioinspir. Biomim.* **3**, 034001.

Hedrick, T. L. and Biewener, A. A. (2007). Low speed maneuvering flight of the rose-breasted cockatoo (*Eolophus roseicapillus*). I. Kinematic and neuromuscular control of turning. *J. Exp. Biol.* **210**, 1897-1911.

Iriarte-Díaz, J. and Swartz, S. M. (2008). Kinematics of slow turn maneuvering in the fruit bat *Cynopterus brachyotis*. *J. Exp. Biol.* **211**, 3478-3489.

Jackson, B. E. and Dial, K. P. (2011). Scaling of mechanical power output during burst escape flight in the Corvidae. *J. Exp. Biol.* **214**, 452-461.

Land, M. F. (1993). Chasing and pursuit in the dolichopodid fly *Poecilobothrus nobilitatus*. *J. Comp. Physiol. A* **173**, 605-613.

Land, M. F. and Collett, T. S. (1974). Chasing behaviour of houseflies (*Fannia canicularis*). *J. Comp. Physiol.* **89**, 331-357.

Lourakis, M. I. and Argyros, A. A. (2009). SBA: A software package for generic sparse bundle adjustment. *ACM Trans. Math. Softw.* **36**, 1-30.

Olberg, R. M., Worthington, A. H. and Venator, K. R. (2000). Prey pursuit and interception in dragonflies. *J. Comp. Physiol. A* **186**, 155-162.

Olberg, R. M., Seaman, R. C., Coats, M. I. and Henry, A. F. (2007). Eye movements and target fixation during dragonfly prey-interception flights. *J. Comp. Physiol. A* **193**, 685-693.

Park, K. J., Rosén, M. and Hedenström, A. (2001). Flight kinematics of the barn swallow (*Hirundo rustica*) over a wide range of speeds in a wind tunnel. *J. Exp. Biol.* **204**, 2741-2750.

Pennycuick, C. J. (1975). Mechanics of flight. In *Avian Biology*, Vol. 5 (ed. D. S. Farner and J. R. King), pp. 1-75. New York, NY: Academic Press.

Petrie, M. and Møller, A. P. (1991). Laying eggs in others' nests: Intraspecific brood parasitism in birds. *Trends Ecol. Evol.* **6**, 315-320.
Pinheiro, J., Bates, D., DebRoy, S., Sarkar, D. and R Core Team (2010). nlme: linear and nonlinear mixed effects models. R package version 3.1-97, http://CRAN.R-project.org/package=nlme.
Portugal, S. J., Hubel, T. Y., Fritz, J., Heese, S., Trobe, D., Voelkl, B., Hailes, S., Wilson, A. M. and Usherwood, J. R. (2014). Upwash exploitation and downwash avoidance by flap phasing in ibis formation flight. *Nature* **505**, 399-402.
R Development Core Team (2010). *R: A Language and Environment for Statistical Computing*. Vienna, Austria: R Foundation for Statistical Computing. Available at: http://www.R-project.org/.
Riskin, D. K., Willis, D. J., Iriarte-Díaz, J., Hedrick, T. L., Kostandov, M., Chen, J., Laidlaw, D. H., Breuer, K. S. and Swartz, S. M. (2008). Quantifying the complexity of bat wing kinematics. *J. Theor. Biol.* **254**, 604-615.
Ros, I. G., Bassman, L. C., Badger, M. A., Pierson, A. N. and Biewener, A. A. (2011). Pigeons steer like helicopters and generate down- and upstroke lift during low speed turns. *Proc. Natl. Acad. Sci. USA* **108**, 19990-19995.
Spedding, G. R., Rosén, M. and Hedenström, A. (2003). A family of vortex wakes generated by a thrush nightingale in free flight in a wind tunnel over its entire natural range of flight speeds. *J. Exp. Biol.* **206**, 2313-2344.
Stiles, F. G., Altshuler, D. L. and Dudley, R. (2005). Wing morphology and flight behavior of some North American hummingbird species. *Auk* **122**, 872-886.
Swaddle, J. P. (1997). Within-individual changes in developmental stability affect flight performance. *Behav. Ecol.* **8**, 601-604.
Tobalske, B. W. (2007). Biomechanics of bird flight. *J. Exp. Biol.* **210**, 3135-3146.
Tobalske, B. and Dial, K. (1996). Flight kinematics of black-billed magpies and pigeons over a wide range of speeds. *J. Exp. Biol.* **199**, 263-280.
Therialt, D. H., Fuller, N. W., Jackson, B. E., Bluhm, E., Evangelista, D., Wu, Z., Betke, M. and Hedrick, T. L. (2014). A protocol and calibration method for accurate multi-camera field videography. *J. Exp. Biol.* **217**, 1843-1848.
Ward, S., Möller, U., Rayner, J. M. V., Jackson, D. M., Bilo, D., Nachtigall, W. and Speakman, J. R. (2001). Metabolic power, mechanical power and efficiency during wind tunnel flight by the European starling *Sturnus vulgaris*. *J. Exp. Biol.* **204**, 3311-3322.
Warrick, D. R. (1998). The turning- and linear-maneuvering performance of birds: the cost of efficiency for coursing insectivores. *Can. J. Zool.* **76**, 1063-1079.
Warrick, D. R., Dial, K. P. and Biewener, A. A. (1998). Asymmetrical force production in the maneuvering flight of pigeons. *Auk* **115**, 916-928.
Zeger, S. L., Liang, K. Y. and Albert, P. S. (1988). Models for longitudinal data: a generalized estimating equation approach. *Biometrics* **44**, 1049-1060.